

Supplemental Information

Cell Metabolism, Volume 13

FGF15/19 Regulates Hepatic Glucose Metabolism by Inhibiting the CREB-PGC-1 α Pathway

Matthew J. Potthoff, Jamie Boney-Montoya, Mihwa Choi, Tianteng He, Nishanth E. Sunny, Santhosh Satapati, Kelly Suino-Powell, H. Eric Xu, Robert D. Gerard, Brian N. Finck, Shawn C. Burgess, David J. Mangelsdorf, and Steven A. Kliewer

Supplemental Experimental Procedures

Microarray analyses

Total liver RNA was isolated from wild-type mice administered vehicle, purified FGF15 or recombinant FGF19 for 6 hr via a jugular vein injection as described (Inagaki et al., 2005). Mice did not have access to food throughout the 6 hr treatment, and livers were harvested and immediately frozen in liquid nitrogen. Microarray analyses were performed using the Mouse Genome 430A 2.0 array (Affymetrix) and results were analyzed using GeneSifter microarray data analysis server (Geospiza).

QPCR

QPCR was performed as described (Potthoff et al., 2009). *Pgc1 α* , *G6pase*, *Pepck*, *ATP5b*, *Cytc*, *Idh3a* and *cyclophilin* primers were as described (Potthoff et al., 2009). *Cyp7a1*, *Acc2*, *Srebp1c*, *Fas*, *Scd1* and *Fgf15* primers were as described (Inagaki et al., 2005; Kalaany et al., 2005).

Immunoblot analysis

Immunoblot analysis was performed as described (Inagaki et al., 2005; Potthoff et al., 2009). Antibodies for phospho-CREB (Ser133) and phospho-CRTC2 were gifts from Dr. Marc Montminy. The PGC-1 α antibody was from Santa Cruz and the β -actin antibody was from Sigma. All other antibodies were from Cell Signaling Technology. All primary antibodies were used in 3% BSA at a dilution of 1:1000 except for phospho-CREB (Ser133), phospho-CRTC2, and β -actin antibodies, which were used at dilutions of 1:2000, 1:5000, and 1:5000, respectively.

ChIP assays

Frozen male adult mouse liver was crushed into powder and equal quantities of each sample were pooled. DNA-protein crosslinking was performed by incubating pooled powdered liver tissue (30 mg) with 1% formaldehyde in PBS containing protease inhibitor cocktail (Roche) and phosphatase inhibitor cocktail (Sigma) for 10–15 min at room temperature with gentle shaking. Crosslinking reactions were stopped by adding glycine to 0.125 M. Liver nuclei were isolated with a dounce homogenizer in hypotonic solution followed by centrifugation at 4000 \times g for 1 min. ChIP assays were performed with liver nuclei using a ChIP assay kit (Millipore) as per the manufacturer's recommendations with anti-AcH3 (Millipore), anti-CREB antibody (Cell Signaling), anti-

CBP (Santa Cruz Biotechnology), anti-PGC-1 α (Santa Cruz Biotechnology) or control rabbit IgG (Cell Signaling). Precipitated DNA was purified using phenol/chloroform extraction and DNA was subjected to QPCR analysis as described (Bookout and Mangelsdorf, 2003). ChIP primers were as follows: *Pgc1 α CRE* -211/-146 FWD, 5'-CAGAGGGCTGCCTTGGA-3', REV, 5'-CAGCCTCCCTTCTCCTGTG-3'; *G6Pase CRE* -179/-110 FWD, 5'-TGTGCCTGTTTTGCTATTTTACG-3', REV, 5'-AAGGTGCATCATCAGTAGGTTGA-3'; *Pepck CRE* -162/-96 FWD, 5'-CCCTGGAGTTTATTGTGTTAAGTCAGT-3', REV, 5'-GCAGGCCTTTGGATCATAGC-3'.

Metabolic parameter measurements

Plasma glucose levels were measured using the glucose autokit (Wako Chemicals Inc.). Plasma triglyceride concentrations were measured using the Infinity triglyceride kit (Thermo Scientific). Plasma β -hydroxybutyrate concentrations were measured using a D-3-hydroxybutyric acid kit (Wako Chemicals Inc.). Plasma insulin levels were measured using the Ultra Sensitive Mouse Insulin Elisa Kit (Crystal Chem Inc.). Plasma cholesterol levels were measured using the Infinity Cholesterol kit (Thermo Scientific). Plasma glucagon levels were measured by immediately adding aprotinin (1000 KIU/mL blood) to blood following collection, and then spinning to collect plasma. Plasma samples were flash frozen in liquid nitrogen and sent to the Vanderbilt Hormone Assay Core for analysis. Total PP1/PP2A phosphatase activity and PP2A phosphatase activity were measured using the Ser/Thr Phosphatase Assay Kit 1 (Millipore) and the PP2A Immunoprecipitation Phosphatase Assay Kit (Millipore), respectively. All measurements were performed following the manufacturer's instructions.

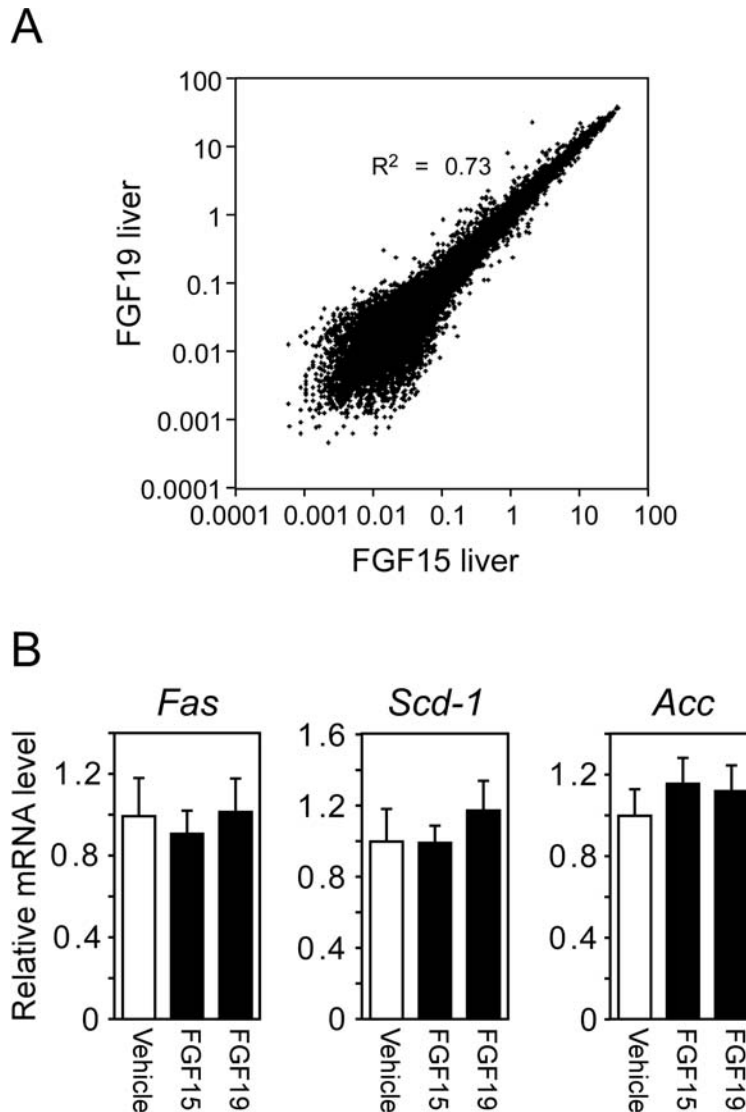


Figure S1, related to Figure 1.

(A) Scatter plot showing relative effects of FGF15 and FGF19 on hepatic gene expression as measured by Affymetrix microarray analysis. Mice ($n = 4/\text{group}$) were injected with vehicle, FGF15 or FGF19 and killed 6 hr later. Mice were fasted during the treatment period. Data were analyzed using a quality call cutoff value of 1 and are plotted as fold regulation by FGF19 (relative to vehicle) on the y-axis versus fold regulation by FGF15 (relative to vehicle) on the x-axis. (B) Hepatic lipogenic gene expression measured by QPCR. Mice ($n = 4/\text{group}$) were injected with vehicle, FGF15 or FGF19 and killed 6 hr later. Mice were fasted during the treatment period. Data are presented as mean \pm SEM.

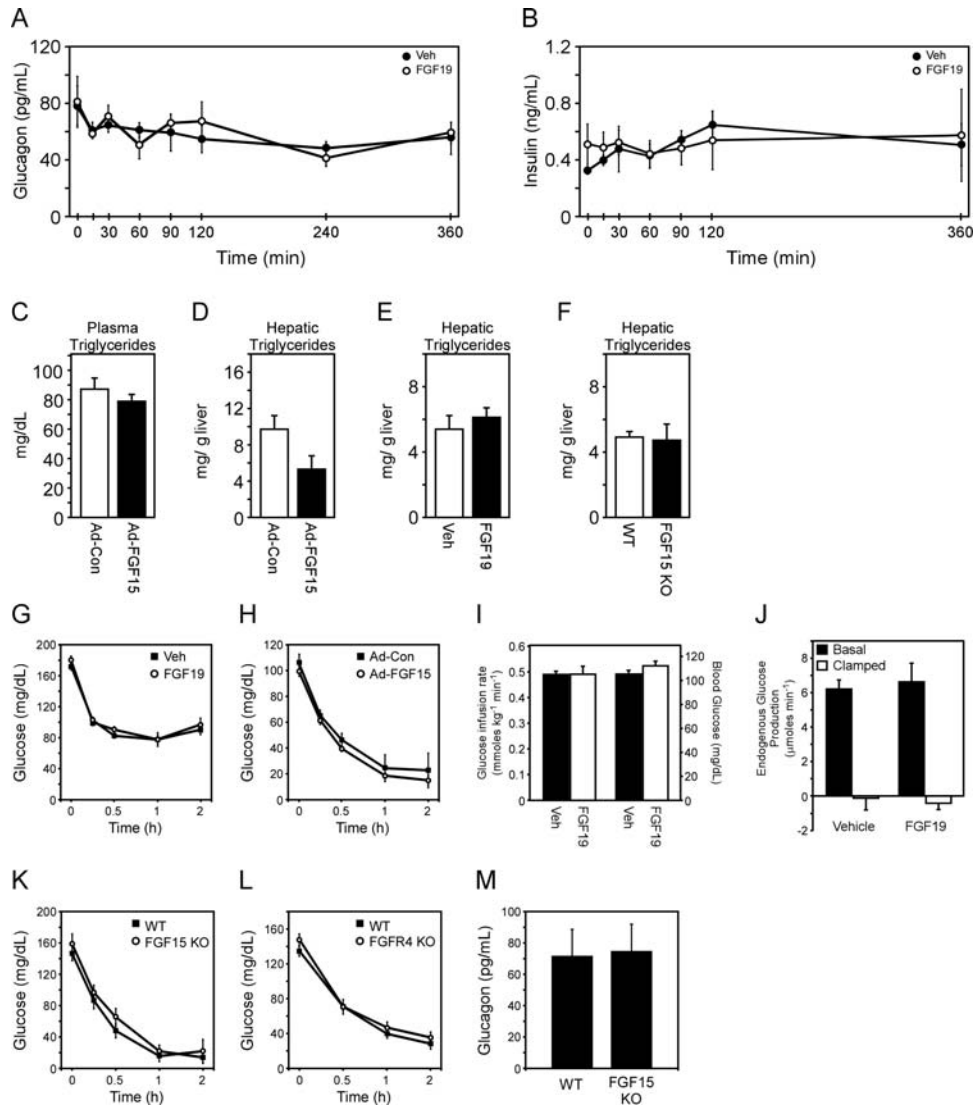


Figure S2, related to Figure 3.

(A-B) Tail blood was collected at the indicated times from wild-type (WT) mice administered vehicle (Veh) or FGF19 and then assayed for plasma glucagon (A) and insulin (B). Mice were fasted during the treatment period. (C-D) Plasma (C) and hepatic (D) triglyceride levels in mice infected with control (Ad-Con) or FGF15-expressing adenovirus (Ad-FGF15) for 3 days and then fasted for 6 hr ($n = 5/\text{group}$). (E-F) Hepatic triglyceride levels in (E) WT C57Bl/6 mice administered Veh or FGF19 and (F) WT and FGF15 KO mice ($n = 5/\text{group}$). (G-H) Insulin tolerance tests in mice treated with (G) FGF19 or vehicle (Veh) or (H) Ad-FGF15 or Ad-Con ($n = 6/\text{group}$). (I-J) Hyperinsulinemic/euglycemic clamps in WT mice administered vehicle (Veh) or FGF19 ($n = 5-6/\text{group}$). (I) Glucose infusion rate and plasma glucose level during the clamp. (J) Endogenous glucose production during basal and clamped conditions. (K-L) Insulin tolerance tests in FGF15-KO (K) and FGFR4-KO (L) mice compared to WT counterparts. (M) Plasma glucagon levels in fed WT and FGF15-KO mice. All data are presented as mean \pm SEM.

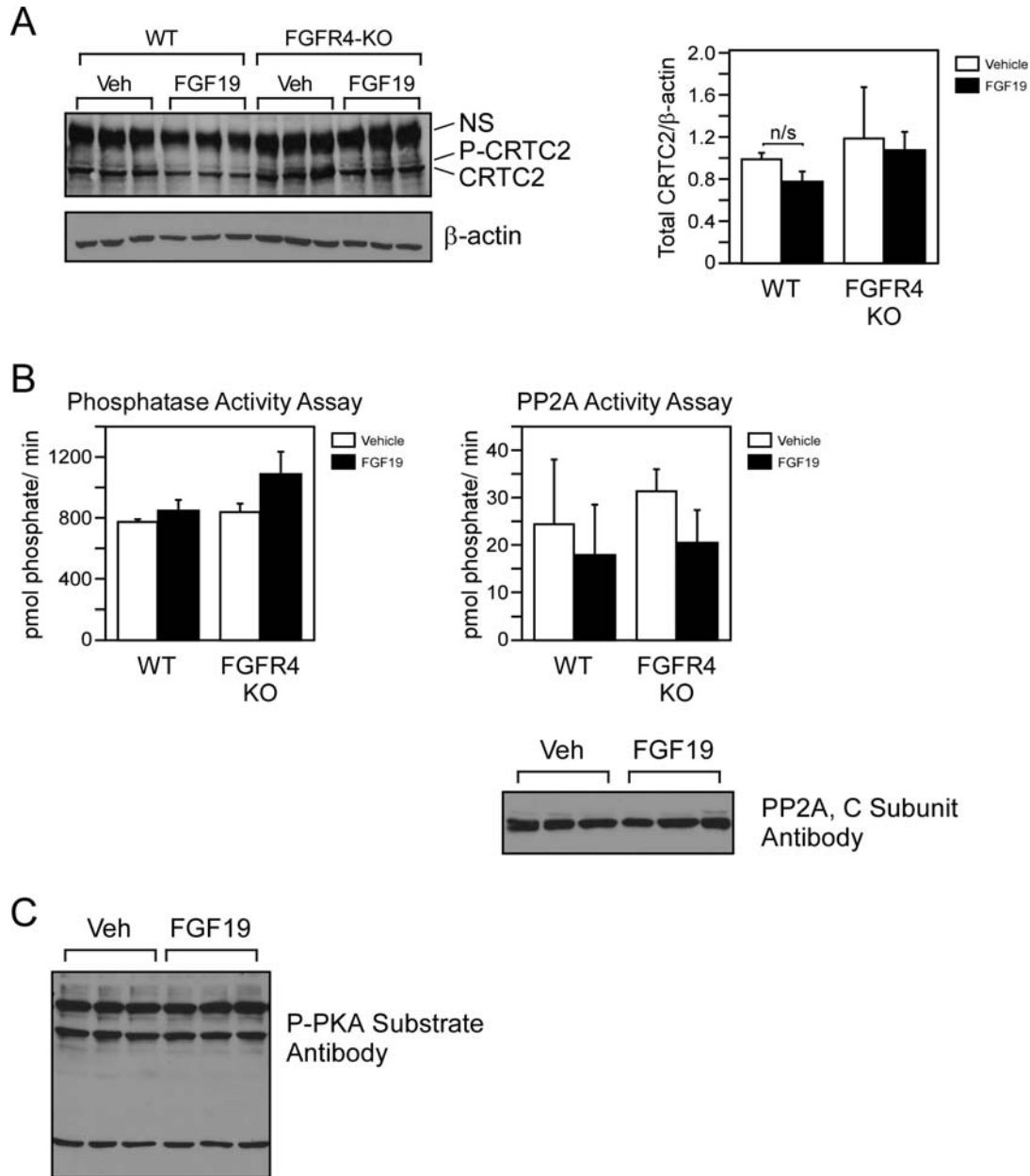


Figure S3, related to Figure 4.

(A, left panel) Western blot analysis and quantification of phosphorylated and unphosphorylated CRTC2 in total liver lysates from individual overnight fasted wild-type (WT) and FGFR4-knockout (KO) mice 30 min after treatment with vehicle or FGF19. NS indicates a non-specific band. β -Actin served as a loading control. Data are quantified in the right panel. (B) Total PP1/PP2A phosphatase activity (left panel), PP2A activity (upper right panel) and PP2A catalytic subunit levels (lower right panel) in liver lysates from individual overnight fasted WT and FGFR4- KO mice ($n = 4$ /group) treated for 30 min with vehicle or FGF19. (C) Western blot analysis of PKA activity using a phospho-PKA substrate antibody and liver lysates from individual overnight fasted WT mice administered either vehicle or FGF19 for 30 min. For bar graphs, data are presented as mean \pm SEM.

Supplemental References

Bookout, A.L., and Mangelsdorf, D.J. (2003). A quantitative real-time PCR protocol for analysis of nuclear receptor signaling pathways. *NURSA e-Journal 1*, ID# 1.11082003.11082001.

Inagaki, T., Choi, M., Moschetta, A., Peng, L., Cummins, C.L., McDonald, J.G., Luo, G., Jones, S.A., Goodwin, B., Richardson, J.A., Gerard, R.D., Repa, J.J., Mangelsdorf, D.J., and Kliewer, S.A. (2005). Fibroblast growth factor 15 functions as an enterohepatic signal to regulate bile acid homeostasis. *Cell Metab 2*, 217-225.

Kalaany, N.Y., Gauthier, K.C., Zavacki, A.M., Mammen, P.P., Kitazume, T., Peterson, J.A., Horton, J.D., Garry, D.J., Bianco, A.C., and Mangelsdorf, D.J. (2005). LXRs regulate the balance between fat storage and oxidation. *Cell Metab 1*, 231-244.

Potthoff, M.J., Inagaki, T., Satapati, S., Ding, X., He, T., Goetz, R., Mohammadi, M., Finck, B.N., Mangelsdorf, D.J., Kliewer, S.A., and Burgess, S.C. (2009). FGF21 induces PGC-1alpha and regulates carbohydrate and fatty acid metabolism during the adaptive starvation response. *Proc Natl Acad Sci U S A 106*, 10853-10858.